Magnetic Structure of LaCrO_{3} Perovskite under High Pressure from In Situ Neutron Diffraction

J.-S. Zhou, J. A. Alonso, A. Muoñz, M. T. Fernández-Díaz, and J. B. Goodenough

Phys. Rev. Lett. **106**, 057201 — Published 31 January 2011

DOI: 10.1103/PhysRevLett.106.057201

Magnetic structure of $LaCrO_3$ perovskite under high pressure from *in-situ* neutron diffraction

J.-S. Zhou [1], J.A. Alonso [2], A. Muñoz [3], M.T. Fernández-Díaz [4], J.B. Goodenough [1]

[1] *Texas Materials Institute, University of Texas at Austin, Austin, Texas 78712 USA*
[2] *Instituto de Ciencia de Materiales de Madrid, CSIC, Cantoblanco, E-28049 Madrid, Spain*
[3] *Dpto. Física Aplicada, EPS, Universidad Carlos III, Avda. Universidad, 30, Leganés-Madrid , E-28911, Spain*
[4] *Institute Laue-Langevin (ILL) 156X, F-38042 Grenoble Cedex 9, France*

The temperature-pressure phase diagram for both the crystal and magnetic structures of $LaCrO_3$ perovskite has been mapped out by *in-situ* neutron diffraction experiments under pressure. The system offers the opportunity to study the evolution of magnetic order, spin direction, and magnetic moment on crossing the orthorhombic/rhombohedral phase boundary. Moreover, a microscopic model of the superexchange interaction has been developed on the basis of the crystal structure obtained in this work to account for the behavior of T_N under high pressure.

Antiferromagnetic ordering lowers the overall symmetry in a magnet. In most cases, magnetic structures can be described by irreducible representations of the symmetry of the crystal structure.[1] Transition-metal oxides with the perovskite structure offer a variety of antiferromagnetic and ferromagnetic spin arrangements on the basis of the 23 tilting systems developed in the structure. [2 3 4] For the tilting system $a^+b^-b^-$ of the Glazer notation and the *Pbnm* space group, the relationship between magnetic structure and crystal structure has been illustrated by Bertaut in the 1960s; [5] he defined the A, G, C and F magnetic modes according to the observed magnetic coupling between the 4 magnetic atoms present in the orthorhombic *Pbnm* unit cell. Among them, the G-type stands for an isotropic antiferromagnetic coupling of a given atom with the six magnetic neighbors. In the presence of an anisotropic exchange interaction or the single-ion anisotropy, a canted-spin structure is developed. All possible canted-spin structures can also be specified in connection with the spin direction by irreducible representations. A huge number of studies in the literature have been focused on the structure with the *Pbnm* space group and its subgroup $P2_1/m$ since the space groups accommodate all antiferromagnetic and ferromagnetic spin-ordering phases.[6] Whereas both antiferromagnetic type-G and ferromagnetic phases have been found in mixed-valent perovskites with the $a^-a^-a^-$ tilting system of the *R-3c* space group, [7 8] it has not been shown whether a single-valent rhombohedral perovskite can also accommodate type-G magnetic ordering.

The *R-3c* space group allows cooperative octahedral-site rotations about the [111] direction of the primary cubic unit cell or the *c* axis in the hexagonal setting. A few perovskite oxides $A^{3+}B^{3+}O_3$ with the geometric tolerance factor $t \equiv (A\text{-}O)/[\sqrt{2}(B\text{-}O)] \leq 1$ adopt the *R-3c* crystal structure at ambient pressure, *e.g.* $RAlO_3$ (R= La, Pr, Nd), $LaCoO_3$, $LaNiO_3$, $LaCuO_3$, $LaGaO_3$ (at $T > 540$ K). However, all these oxides are non-magnetic. The rhombohedral (R) phase can also be stabilized under pressure, which increases the possibility to convert some magnetic perovskites with orthorhombic (O) structure into the R phase. The crystal structure of $LaMnO_3$ under 12 GPa has been refined well with the *R-3c* symmetry from x-ray diffraction data. [9] Unfortunately, the type-A antiferromagnetic phase collapses at the phase boundary because the structure of the R phase is not compatible with the Jahn-Teller (JT) distortion; an orbital ordering is

required for the magnetic coupling in this JT-active system. The O/R phase transition in $LaFeO_3$ occurs at 1200 K, [10] which is much higher than the Néel temperature $T_N \approx 740$ K.[10] Although T_N increases under pressure, it never meets the O/R phase boundary since a spin-state transition is induced at higher pressure.[11] In the perovskite nickelates $PrNiO_3$, the first-order metal-insulator/magnetic transition is completely suppressed under pressure before the O/R phase transition takes place.[12] The O phase of $LaCrO_3$ with the type-G antiferromagnetic spin ordering below T_N is perhaps the only candidate for us to explore how the magnetic phase enters the R phase under high pressure. The pressure-induced orthorhombic-to-rhombohedral (O/R) phase transition at $P \approx 5.0$ GPa has been revealed by synchrotron diffraction studies under high-pressure.[13] [14] Since the O/R transition at $T_t \approx 540$ K [14] under ambient pressure can be continuously reduced to room temperature under 5 GPa whereas $T_N = 298$ K at ambient pressure is expected to increase under pressure in this localized spin system, T_N may cross T_t at $P \geq 5$ GPa. Therefore, a magnetic structure study can reveal whether the type-G spin ordering collapses at T_t. However, previous studies with synchrotron diffraction and a diamond-anvil cell did not provide any information about the magnetic structure. A high-pressure neutron-diffraction study is needed for this task.

In this work, we have carried out an *in-situ* neutron powder diffraction investigation of the P-T phase diagram of $LaCrO_3$ with a Paris-Edinburgh (P-E) cell.[15] This device incorporates a large-volume, liquid-filled chamber suitable for studying structural and magnetic structures with neutrons. Advantages from the P-E device come at a price; operating a massive P-E device at cryogenic temperatures is extremely time consuming and the highest pressure is about 10 GPa. Since the high-pressure study of crystal and magnetic structures of $LaCrO_3$ can be done around 6 GPa near room temperature, these drawbacks were largely avoided.

$LaCrO_3$ has been synthesized by firing a mixture of La_2O_3 and Cr_2O_3 in the temperature range 950-1500° C in air with several intermediate grindings. Neutron powder diffraction (NPD) experiments under high pressure were performed at the high-flux D20 diffractometer of the Institut Laue-Langevin (ILL) in Grenoble, France. The high-

resolution mode (take-off angle of 120º) was selected with a wavelength 1.866(1) Å. The sample, mixed with NaCl powder as the pressure manometer, was loaded into an encapsulated TiZr gasket filled with a 4:1 mixture of methanol-ethanol as a pressure medium before pressing in a P-E device. The loading force was kept constant during cooling of the sample. The NPD patterns were analyzed by the Rietveld method with the FULLPROF program.

A pressure scan at room temperature was first performed; NPD patterns were collected at pressure points 0.06, 0.70, 2.18, 4.00, 5.49, 5.79, 5.97 and 6.59 GPa. Fig. 1 illustrates the quality of the NPD patterns of the O phase (P= 2.18 GPa) and the R phase (P= 5.97 GPa). The three series of Bragg reflections correspond to the main crystallographic phase, NaCl, and the magnetic structure. Fig. 2(a) shows the pressure dependences of lattice parameters at room temperature. The O/R phase transition occurs at $P_c \approx 5$ GPa where we have observed the two-phase coexistence; at P = 5.5 GPa, the refinement shows 90(1)% R phase in the sample. Results of refining NPD data for both O and R structures under high pressure at room temperature can be found in Tables S1 and S2 in Supplementary Materials. The *Pbnm* space group requires $b > a$ for rigid octahedra. However, the local site distortion, characterized by the O_{22}-Cr-O_{21} bond angle $\alpha \leq 90$ ° that sets in from $GdCrO_3$ as the rare earth R^{3+} ionic radius increases in the $RCrO_3$ family,[16 17] reduces lattice parameter *b* and eventually makes $b < a$ for $LaCrO_3$. High pressure appears to continuously increase $a - b$ by further enlarging the local distortion although the resolution of our neutron diffraction is insufficient to resolve the pressure-induced change in the bond angle α within 1 degree. The first-order transition to the *R-3c* phase occurs because the cubic phase cannot be achieved by continuously reducing the octahedral-site rotations in the O phase.[16] Moreover, the *Pbnm* space group is not a subgroup of the *R-3c* space group. A phase transition between these two space groups cannot be driven by continuously changing the tilting components. Since both structures consist of corner-shared octahedra, we are able to track down the changes of lattice parameters on crossing the phase transition through the relationship between these two unit cells. The most obvious change in the lattice parameters on passing P_c is along the *c* axis of the *Pbnm* cell. Fitting the V versus P curve with a third-order Birch-Murnagham equation of state

gives a bulk modulus B = 188 ±2 GPa (B' = 4 fixed) for the O phase. We can also determine pressure-induced changes of atomic positions from the refinements. Fig. 2(b) shows that the averaged Cr-O bond length shrinks almost continuously whereas a small jump of the Cr-O-Cr bond angle can be clearly seen on passing P_c as pressure increases.

Peaks of magnetic origin can be discerned at room temperature for $P \geq 2.2$ GPa, indicative of a $T_N > 300$ K. The inset of Fig. 1 highlights the main magnetic reflection in O and R phases; in both phases the propagation vector is $k = 0$. The magnetic structure of the O phase $LaCrO_3$ developed at ambient pressure has been refined in the G_x mode.[6] As for the R phase, the group theory admits three possible magnetic structures compatible with the *R-3c* symmetry and k=0. The fit for the G_z structure is excellent with a discrepancy factor R_{mag} of 11.4 %. The results of refinements with all three possible magnetic structures can be found in Supplementary Material. In order to follow the thermal evolution of crystal and magnetic structures and to map out T_t in the T-P phase diagram, we collected neutron diffraction data while cooling down the sample at P = 2.2, 5.5, and 6.6 GPa. A first-order transition to reenter the O phase occurs at $T_t = 262$ K under 5.5 GPa. Fig. S2 in supplementary material illustrates a characteristic range of the NPD patterns where the progression of the R/O transition is clearly followed upon cooling across the R/O boundary at 5.5 GPa. The same phase transition was observed at even lower temperature, $T_t = 175$ K under 6.6 GPa. A linear decrease of T_t versus P with a $dT_t/dP = -48.2 \pm 0.9$ K can be obtained in Fig.2(c) from these data and T_t at ambient pressure from the literature.[14]

Fig.3 shows the temperature dependence of the ordered magnetic moment M(T) at Cr^{3+} under three pressures. Fitting these data with the Brillouin function gives T_N and the magnetic moment M_0 at zero Kelvin. The R/O phase transition causes a discontinuous change at T_t, which can be seen clearly in the curve of M(T) under P=5.5 GPa. The curve fitting at P = 5.5 GPa was made to data points within the R phase shown in the inset of Fig.3. Data points in the O phase point to a slightly lower T_N than that in the R phase at P = 5.5 GPa. It is important to know that the curve fittings to the data of both the O phase under P = 2.17 GPa and the R phase under P =5.5 GPa give an $M_0 = 3.0\ \mu_B$/Cr, which

indicates that a localized electron model remains applicable in the O and R phases. Although T_N increases progressively under pressure, M_0 for the M(T) curve under P =6.6 GPa is clearly lower than those at lower pressures. This issue will be discussed in connection with the breakdown of the localized electron model. As mapped in Fig. 2(c), T_N increases with pressure nearly linearly to P =5.6 GPa and does not show a jump at the O/R phase boundary. T_N at 6.6 GPa clearly deviates from the line of T_N versus P obtained at lower pressures. To reveal the pressure dependences of T_N and T_t is only the first step in this study. The *in-situ* neutron diffraction data under pressure also provide information for us to study the change of spin structure on crossing the O/R phase boundary and to test whether the superexchange formula can account for the pressure dependence of T_N on the basis of crystal-structure changes.

The superexchange interaction theory gives a relationship between the magnetic-coupling parameter J and the orbital overlap integral b by $J \propto b^2/U$, where U is the on-site Coulomb energy. The Néel temperature can be calculated through a mean-field formula $k_B T_N = 4S(S+1)J$, S is the total spin on a magnetic ion. The detailed correlation between the orbital overlap integral b and the average Cr-O bond length r and the average Cr-O-Cr bond angle θ ($\omega = 180° - \theta$) has been recently worked out and tested for a t^3 system like that of the $RCrO_3$ family.[17]

$$J = J_0[(b^{\pi})^2 - 1.5(b^{\sigma}_{hb})^2]/r^7,\ \ b^{\pi} = 2(\sin(\omega/2)+\cos(\omega/2))-4\sin(\omega/2)\cos^2(\omega/2),$$
$$b^{\sigma}_{hb} =[\sin(\omega/2)+\cos(\omega/2)]*[\sqrt{3}\sin(\omega/2)\cos(\omega/2) + \sqrt{3}/2(\cos^2(\omega/2) - \sin^2(\omega/2) - 1/2], \quad (1)$$

where J_0 includes the angle-independent overlap integral and U. The term b^{π} is the angle-dependent overlap integral through the π bond and the term b^{σ}_{hb} is a correction due to the orbital hybridization with the σ bond. By using the structural data in Fig.2, we can calculate the pressure dependence of the normalized T_N as a function of pressure in Fig.2(d). This microscopic model works reasonably well to catch the essential feature of T_N(P) observed. Although a jump of T_N at T_t predicted from the calculation is absent in the T_N(P) which was obtained through fitting the M(T) data, a fitting that may not convey sufficient resolution, a discontinuous change in M(T) at T_t under 5.5 GPa of Fig.3 indicates clearly a slightly higher T_N in the R phase than that in the O phase. We have also compared two outputs from calculations with/without the π–σ orbital-hybridization

effect. The hybridization plays an essential role to account for the overall change of T_N as a function of the rare-earth ionic radius in the $RCrO_3$ family.[17] The calculation by including the correction also brings the calculated T_N one step closer to T_N observed. At T_t, the calculation with the correction predicts a larger jump of T_N since the hybridization effect is more sensitive to the change of the Cr-O-Cr bond angle.

Long before the microscopic model, Bloch [18] put forward a phenomenological rule on the basis of experimental results of antiferromagnetic transition-metal oxides. The rule states the following

$$\alpha \equiv (d\ln T_N/dP)/\kappa \approx 3.3 \qquad (2)$$

where the compressibility κ can be calculated from the equation of state. Based on the $\kappa = 5.3 * 10^{-3}$ $(GPa)^{-1}$ from this work, we have calculated the T_{N_Bloch} in Fig.2(c). The prediction based on the Bloch rule fits the $T_N(P)$ data well for $P \leq 6$ GPa. In the perovskite structure, the orbital overlap integral b as described in Eq.1 is related to the bond length and the bond angle, not directly related to the cell volume. It remains open why the Bloch rule based on the volume change can account for the pressure dependence of T_N in the perovskite $LaCrO_3$.

Although the microscopic model and the Bloch rule work successfully at low pressures, neither can account for a dramatic T_N jump at 6.6 GPa. A significant deviation from the Bloch rule has been observed in systems like $LaMnO_3$ [19] and $SmNiO_3$.[20] Deviation from the Bloch rule can be caused either by the breakdown of the perturbation expression of the superexchange interaction or by a volume change that is no longer correlated to the change of the orbital overlap integral. In the case of perovskite $LaCrO_3$, failure of the microscopic model suggests that the localized electronic state is at the brink of collapse under 6.6 GPa. Corresponding to a T_N jump, the M_0 of $LaCrO_3$ also shows a noticeable reduction, which is consistent with a collapsing of the localized electronic state at Cr^{3+}. This argument deserves to be verified by other experimental probes under high pressure.

The orthorhombic $LaCrO_3$ perovskite exhibits the type-G antiferromagnetic spin order at ambient pressure, which is consistent with the superexchange rules for t^3-O-t^3 coupling.

However, the spin ordering direction is degenerate. The group theory set by Bertaut gives two possible configurations for type-G spin order in the *Pbnm* space group, *i.e.* (F_x, C_y, G_z) or (G_x, A_y, F_z). Magnetic susceptibility $\chi(T)$ is the most sensitive probe to detect spin canting. Instead of a cusp at T_N, $\chi(T)$ of $LaCrO_3$, shown as an insert in Fig.4, exhibits a ferromagnetic-like transition at T_N, which is conclusive evidence for canted-spin ordering; the sharpness of $\chi(T)$ near T_N is proportional to the magnitude of the single-ion anisotropy and Dzialoshinski vector **D**.[21] However, the anomaly of $\chi(T)$ does not distinguish these two modes. Refinements of the magnetic structure from NPD data under pressure in the orthorhombic phase do not discriminate these two configurations sharply; refinements with both modes give $R_{mag} \sim 17\%$. We have chosen the solution (G_x, A_y, F_z) here since the mode (F_x, C_y, G_z) aligns spins facing each other at neighboring sites along the *c* axis. This mode occurs only in the case where the rare-earth ion R is magnetic or the octahedral-site is highly distorted. Spins in the (G_x, A_y, F_z) mode are pointed to the octahedral edge in the O_{22}-Cr-O_{21} plane as illustrated in Fig.4(a). The spin canting direction allowed by the symmetry follows the cooperative octahedral-site rotation, which gives the ferromagnetic component along the *c* axis. The spin reorientation on crossing the O/R phase transition in $LaCrO_3$ under high pressure provides a nice example of the relationship between the crystal symmetry and magnetic structure. Although the localized electron model describing the exchange interaction through the t^3-O-t^3 in the perovskite $LaCrO_3$ remains valid on crossing the phase transition, the *R-3c* group symmetry only allows the antiferromagnetic spin structure with the spin direction along the c axis, *i.e.* the axis of highest rotation symmetry in this space group. Therefore, on crossing the O/R phase boundary, the spin direction in the type-G antiferromagnetic phase rotates from pointing to the octahedral edge to perpendicular to the triangle plane of an octahedron in Fig.4. In sharp contrast, the O/R phase transition terminates the antiferromagnetic exchange interaction in $LaMnO_3$ and ferromagnetic exchange interaction in $LaMn_{0.5}Ga_{0.5}O_3$ where long-range magnetic order requires long-range orbital order.[9] Cooperative orbital ordering giving rise to the magnetic coupling for type-A spin ordering in $LaMnO_3$ and for ferromagnetic spin ordering in $LaMn_{0.5}Ga_{0.5}O_3$ is forbidden in the R phase where the structure symmetry allows only one M-O bond length.

In conclusion, the evolution of crystal and magnetic structures of the perovskite $LaCrO_3$ as a function of pressure have been studied by neutron diffraction. At room temperature, $LaCrO_3$ undergoes a first-order structural transition from the orthorhombic *Pbnm* phase to the rhombohedral *R-3c* phase under $P_c \approx 5$ GPa. The phase transition temperature T_t has also been determined at different pressures, which allows us to map out a temperature-pressure phase diagram of the crystal and magnetic structure for $LaCrO_3$. T_t decreases linearly as pressure increases with a slope $dT_t/dP = -48.2$ K/GPa. On crossing the O/R phase transition, the symmetry change of the crystal structure does not alter the localized-electron regime and type-G antiferromagnetism, but it causes a spin reorientation from the spin direction pointing to the edge to that pointing to the triangle face of an octahedron. The possibility of canting the spin structure of the *Pbnm* phase is eliminated in the *R3-c* phase. This study has revealed a rule for spin direction in antiferromagnetic perovskites RMO_3: (1) it is parallel to the rotation axis with the highest symmetry in the space group; (2) if there are more than one rotation axis in the space group, it is determined by either higher-order orbital angular momentum or the R-M exchange interaction for the magnetic rare earth. The behavior of the antiferromagnetic transition temperature T_N under high pressure in both the O and R phases can be quantitatively accounted for either by a microscopic superexchange model based on the crystal structure obtained from this study or by a phenomenological Bloch rule for $P < 6$ GPa. A dramatic increase of T_N accompanied by a clear reduction of magnetic moment in the R phase under $P \geq 6.5$ GPa signals a breakdown of the localized-electron picture in $LaCrO_3$.

Acknowledgment
This work was supported by NSF (DMR 0904282) and the Robert A Welch foundation (Grant F-1066), as well as the Spanish Ministry of Science and Innovation (MAT2010-16404).

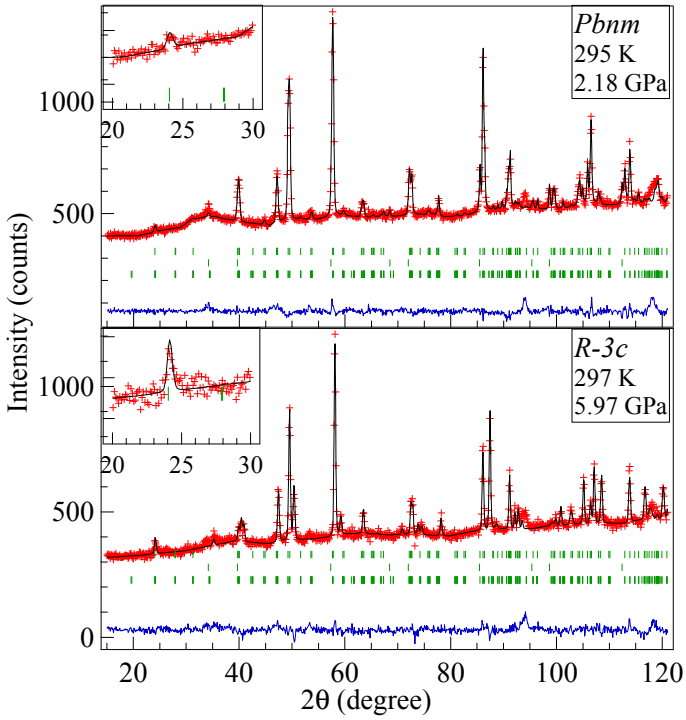

Fig. 1: Observed (crosses), calculated (full line) and difference NPD profiles for $LaCrO_3$ collected at 2.18 GPa and 5.97 GPa at room temperature. The three sets of Bragg reflections correspond to the main crystallographic phase, NaCl, and the magnetic phase. The insets show the main magnetic reflection. Small peaks near 2θ = 94° and 118º come from the TiZr gasket.

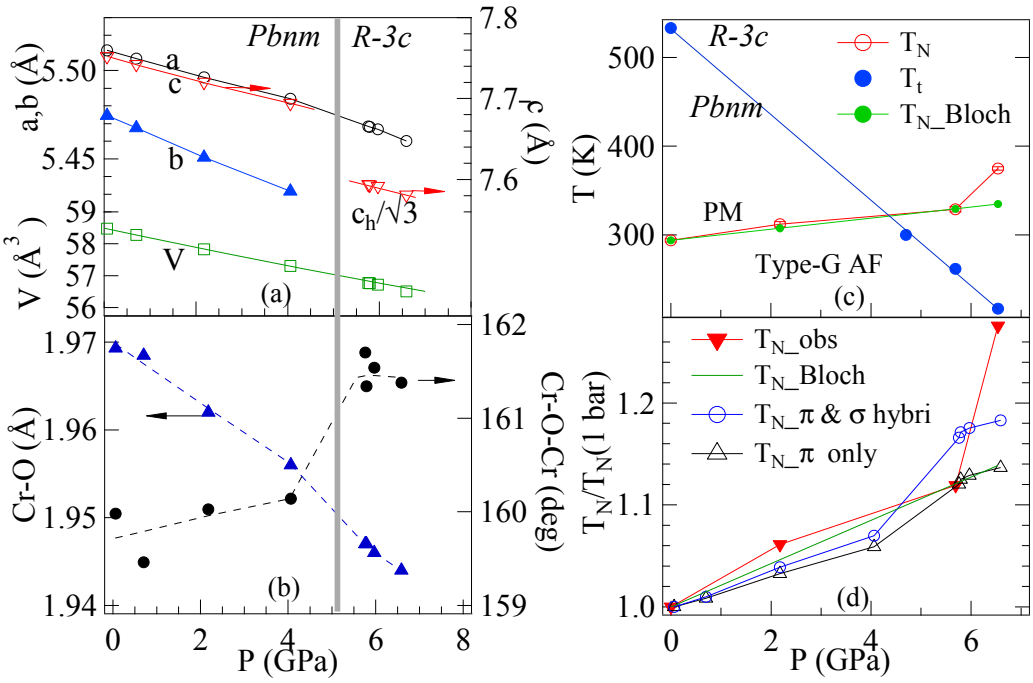

Fig.2 (a,b) Pressure dependences of lattice parameters and the average Cr-O bond length and Cr-O-Cr bond angle of $LaCrO_3$ at room temperature. Dashed lines inside the figure are guide to eyes; instead of raw data, data along dashed lines are used to build a microscopic model to account for the behavior of T_N under pressure. (c) The temperature-pressure phase diagram and (b) the renormalized T_N and values calculated by a microscopic model and the Bloch rule for $LaCrO_3$.

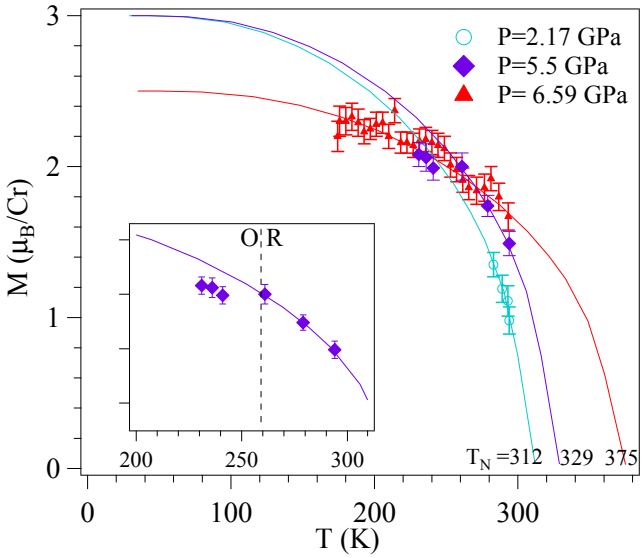

Fig.3 Temperature dependence of magnetic moment M at Cr^{3+} under three different pressures; the inset shows the blow-up plot of M(T) under P = 5.5 GPa. Solid lines inside the figure are curve fittings to the Brillouin function.

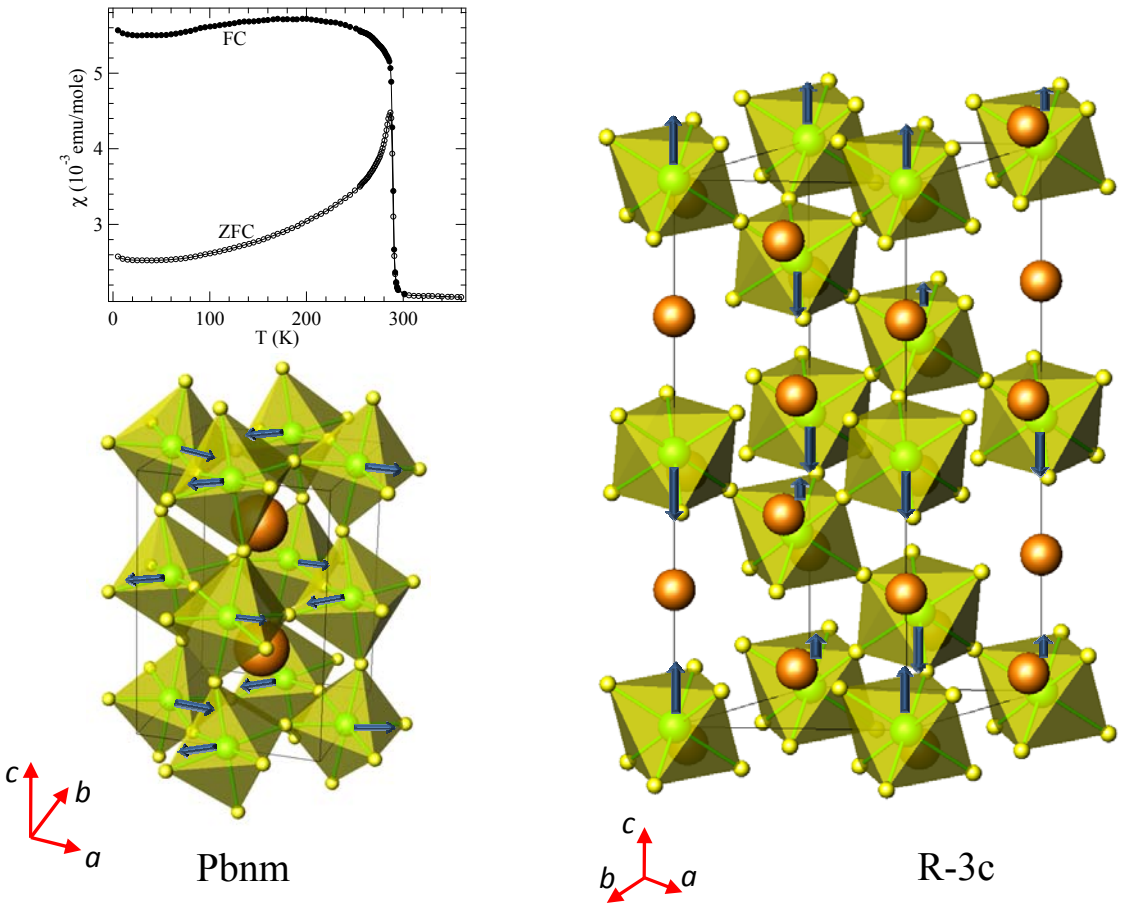

Fig.4 Crystal structures of *Pbnm* and *R-3c* phases with corresponding spin ordering at Cr^{3+} ions. The insert: temperature dependence of the magnetic susceptibility of $LaCrO_3$. The magnitude of spin canting in the *Pbnm* phase is exaggerated for clarification.

jszhou@mail.utexas.edu

[1] Yu A. Izyumov, Sov. Phys. Usp **23**, 356 (1980).
[2] R. H. Mitchell, *Perovskites, Modern and Ancient* (Almaz Press, Ontario, 2002)
[3] E. O. Wollan and W. C. Koehler, Phys. Rev. **100**, 545 (1955).

[4] J. Rodriguez-Carvajal, *et al,* Phys. Rev. B **57**, 456 (1998).
[5] E. F. Bertaut, in *Magnetism*, edited by G. T. Rado and H. Suhl (AP, New York, 1963), Vol. **III**, p.149.
[6] J. B. Goodenough and J. M. Longo, in *Landolt-Bornstein, Crystallorgraphic and magnetic properties of perovskite and perovskite-related compounds*, edited by K.-H. Hellwege (Springer-Verlag, Berlin, 1970), Vol. **4a**, Chap. Group III, p.126.
[7] K. Tezuka, *et al*, J. Solid State Chem. **141**, 404 (1998).
[8] A. Urushibara, *et al*, Phys. Rev. B **51**, 14103 (1995).
[9] J.-S. Zhou, *et al*, Phys. Rev. B **78**, 220402(R) (2008).
[10] R. Dogra, *et al* , Phys. Rev. B **63**, 224104 (2001).
[11] W. M. Xu, *et al*, Phys. Rev. B **64**, 094411 (2001).
[12] J.-S. Zhou, J. B. Goodenough, and B. Dabrowski, Phys. Rev. Lett. **94**, 226602 (2005).
[13] T. Hashimoto, *et al* , Solid State Comm. **108**, 691 (1998).
[14] T. Shibasaki, *et al*, J. Thermal analysis and Calorimetry **81**, 575 (2005).
[15] S. Klotz, *et al*, High Pressure Research **14**, 249 (1996).
[16] J.-S. Zhou and J. B. Goodenough, Phys. Rev. Lett. **94**, 065501 (2005).
[17] J.-S. Zhou, *et al*, Phys. Rev. B **81**, 214115 (2010).
[18] D. Bloch, J. Phys. Chem. Solids **27**, 881 (1966).
[19] J.-S. Zhou and J. B. Goodenough, Phys. Rev. Lett. **89**, 087201 (2002).
[20] J.-S. Zhou, J. B. Goodenough, and B. Dabrowski, Phys. Rev. Lett. **95**, 127204 (2005).
[21] T. Moriya, in *Magnetism*, Ed. by G. T. Rado and H. Suhl (AP, NY, 1963), Vol. **I**, p.3.